Send Orders for Reprints to reprints@benthamscience.ae

Micro and Nanosystems, **2015**, *7*, 31-35

Dynamic Impedance Distribution of Nanoscale Electrodes: Fabrication and Characterization

Thikra S. Dhahi*

Physics Department, College of Education for Pure Science, Basra University, Basra, Iraq

Thikra S. Dhahi

Abstract: Nanogap electrodes fabricated from metals separated by a distance on nanometer scale have gained tremendous acceptance in various fields of applications and essential elements of nanoscale biosensor transducers and electrochemical sensing element. Electrical conduction of nanogap is typically determined by the characteristics of its electron transport molecules and mainly conducted through current-voltage (I-V) measurements. However, due to capacitively shifting behavior of the nanogap device as a result of atomic agintation by the increase in frequency, it is difficult to measure two devices of the same configuration that produce exact behavior. In order to understand these fundamentals, three gap electrodes of three different materials were fabricated and tested for their impedance behavior to identify sensitive and stable atomic configuration mode for maximum detection throughput.

Keywords: Dynamic distribution, gold, nanogap, nanoscale electrode, polysilicon, silicon.

INTRODUCTION

Nanogaps are semiconducto or metallic electrodes separated by space ranging from less than 1nm to 100 nanometers [1, 2]. These structures can be typically used for many applications, especially where studying the electrical properties of single molecule is necessary. The surface modification will be perfomerd to change the device surface profile for possible attachement probing atom and molecule of interest is located in the gap between the two electrodes, for subsequent detection of incoming complement atom [3]. With the interaction of probing atom and incoming atom, electrical profile will be monitored and electrical conduction of nanogap is typically determined by the characteristics of its electron transport molecules and mainly conducted through current-voltage (I-V) measurements. However, due to capacitively shifting behavior of the device as produced from the atomic agintation by the increase in frequency [4, 5], it is difficult to measure two devices of the same configuration that produce similar behavior. In trying to understand these fundamentals, three gap electrodes of three different materials were fabricated and tested for their impendence behavior to identify sensitive and stable atomic configuration mode for maximum detection throughput. In the quest of extremely small nanogaps such in the range of atomic size, it is clear that nanogap with stable behavior is necessary for the possibility of single molecule response achievement [6, 7]. Many researchers argue that increased electric field enhancement might reduce the stability of the system to the point of being unstable to measure, thus leading to searching and checking for more stable materials for optimum operation in different conditions and applications [8]. As a biosensor, however, reaching nanogaps with extreme small size is necessary to detect single molecule. In the scenario of earlier cancer detection among biotechnology based researchers, it has been concluded that for the detection of such entity, extreme nanostructure is necessary and more sensitive multiple molecules detection can envision small size sensor [9-11], The ability to stabilize and produce extremely small nanostructure would make the bio and chemical detection significantly easier, while still being sensitive to very low concentrations of the molecule of interest [12]. The study demonstrates the characterization of three different configurations of nanogap at high frequencies and to determine frequency behavior differences at the sub-nanometer scale and materials, silicon and polysilicon gaps were formed by photolithography and gold nanogaps were formed by chemical reaction coupled with measurements of the nanogap distance. In order to understand the effect of frequencies, the nanogap configurations were tested with ac mode because alternative current (ac) transports behave in a different manner from direct current (dc) transport. In dc transport, current is steady not only in time, but also in position along the transport direction so this will not explain the full device behavior in terms of time and position and currents through any cross-areas are the same no matter in the infinite electrodes. However, in ac transport, current is changing not only in time, but also in position along the transport direction. Ac currents, through different cross-areas in electrodes, are generally different because of charge accumulation and static potential [13, 14].

MATERIALS AND METHODS

The fabrication was started with the electrode pattern and the design was performed by using AUTOCAD for precise geometry and it subsequently transferred binary chrome

*Address correspondence to this author at the Institute of nanoelctronic engineering, University Malaysia Perlis, Perlis, Malaysia;
Tel: 00964-771-678-6725; E-mail: Sthikra@yahoo.com

1876-4037/15 $58.00+.00

marks for pattern transfer. The fabrication is divided according to two approaches, semiconductor based approach for the fabrication of silicon based structures, and chemical based approach for the fabrication of the metallic electrodes. For the semiconductor fabrication process, the device was realized by using 300nm oxide deposited silicon substrate. After two steps (R2 &R1) of cleaning the substrate using HS-3624 ultrasonic machine, EZP520-87 resist is diluted in anisole is spin coated at speed (500rpm) and 200nm thickness was resist obtained after baked at 100 ˚C for 1 minutes. The electrode pad and gap line are then patterned using reactive ion etcher. In the electrodes electrical measurements, we used two electrodes separated by a gap distance by using three materials, namely: gold, silicon and polysilicon. These gap distances were experimentally found to be between 3nm to 15nm for gold materials, 6 to 86nm for silicon, and 5 to 7nm for polysilicon. These achieved sizes were comparable to the size of the nucleotide molecules that can readily be employed in bio-molecular detection. The gap sizes were all reproducible and following method employed photolithographically fabricated gold, silicon and polysilicon nanogap on a thin oxide-deposited silicon substrate, a field emission scanning electron microscope (FESEM) image of typical fabricated nanogaps. The reproducible fabrication procedures for the lithographically defined gap electrode are described in our previous publication in detail [9]. Therefore, to determine the nanogap electrical behavior using impedance as a preliminary understanding of whether the stables are done by determining profile of the device.

$$V = IZ = I\left|Z\right|e^{j\arg(Z)}$$

RESULTS AND DISUSSIONS

Electrical impedance is the measure of the opposition that a circuit presents to a current when a voltage is applied when dealing with dc. When a circuit is driven with direct current (dc), there is no distinction between impedance and resistance, and the dc is thought of as impedance with zero phase angle.

The nanogap more or less behaves as a capacitor and indeed as a super capacitor for that matter, therefore, it is suitable to measure through the dielectric analyzer and dielectric analyzer was setup to measure various parameters and these include the capacitance, loss tangent, conductance, permittivity, etc. The frequencies were swept from 10^{-1}Hz to 10^{7}Hz using dielectric analyzer with AC Volt [Vrms]= 0.400 or 20mV input signal (0 V D.C Offset) Fig. (**1**). The set up reference plane was fully calibrated with reference plane and probing station was fully vacuumed to make a smooth and reliable measurement. Below are typical nanogap measured results for the three materials showing their permittivity linearly dropping as the frequency increases. This behavior could be due to the agitation of electron potential transition, however, the silicon and poly-Si materials actually deviate from actual model, which might be due to lack of supply vacuum where semiconductor electron recovery is slower as compared to metals (Fig. **3**).

The nanogap capacitance model value shown in Fig. (**4**) is 6 nm, and 9nm gap as shown in Fig. (**2**) in the method section. The device was measured for loss angle for air from 10^{0} to 10^{3} and below 10^{-1} Hz as shown in Fig. (**4**). Between 10^{0} and 10^{4} Hz, the factor that ultimately determines the best capacitor is the loss lying between these values. It is worthy to note that the presence of frequency differences and the inverse power dependence of the capacitance with the frequency at the whole range, initially, first decline value as frequency increase indicate the electrode nanogap and the probe contact resistance fluctuation. The gap owns it own really has no ions. The presence of any foreign object reorients the electron flow. For example, DI water is free of ions but ofcourse it still has about 10^{-7} molar each of H+ and OH- ions similar to pH 7, at room temperature. In the ac field, each H_2O dipole changes orientation with the field. If the frequency of the electric field is increased, eventually it becomes so high that the water dipoles cannot turn fast enough to keep up. Then, all that happens is that nuclei and the electron cloud of each water molecule move a little in response to the field. Measured at a very high frequency, water molecules are not free to rotate. Therefore, this device is only valid at low frequency up to 1Mhz.

It can be observed from Fig. (**5**) that at frequencies higher than 10 kHz, the spectrum is dominated by the contribution of the external cell connections, which brought about impendence getting reduced gradually until 10Mhz, where the effect of the impedance no longer exists. This indicated that the electronic conduction between the gap and the active

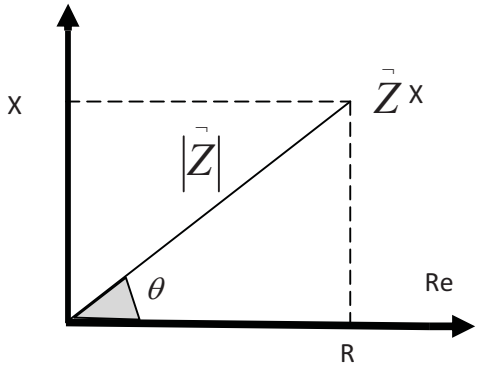

(a)

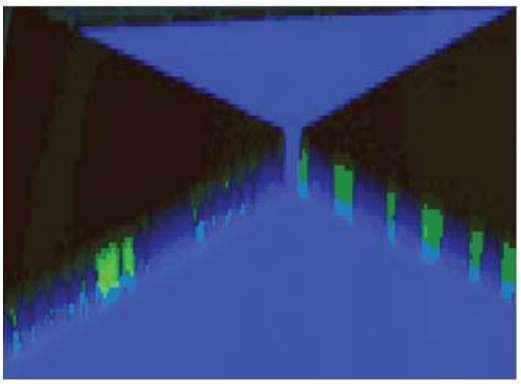

(b)

Fig. (1). (**a**) Showing parametric relationship of the magnitude of the impedance $|Z|$ acting just like the resistance which gives the drop in voltage amplitude across an impedance Z for a given current I, (**b**) illustration of nanogap structure.

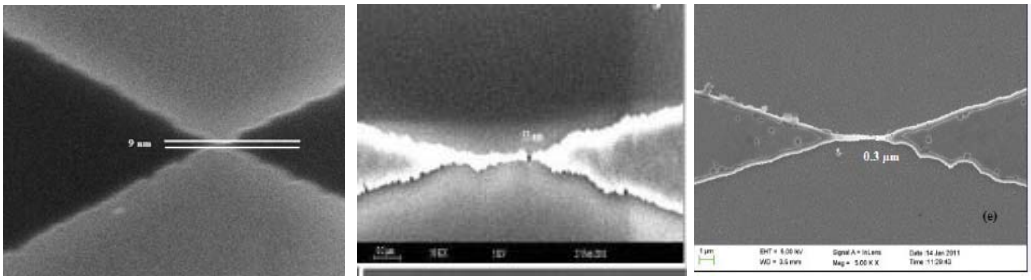

(a) (gold) (b) (silicon) (c) (polysilicon)

Fig. (2). Gold, silicon, poly-Si nanogap structures fabricated using enhanced photolithography and chemical etching.

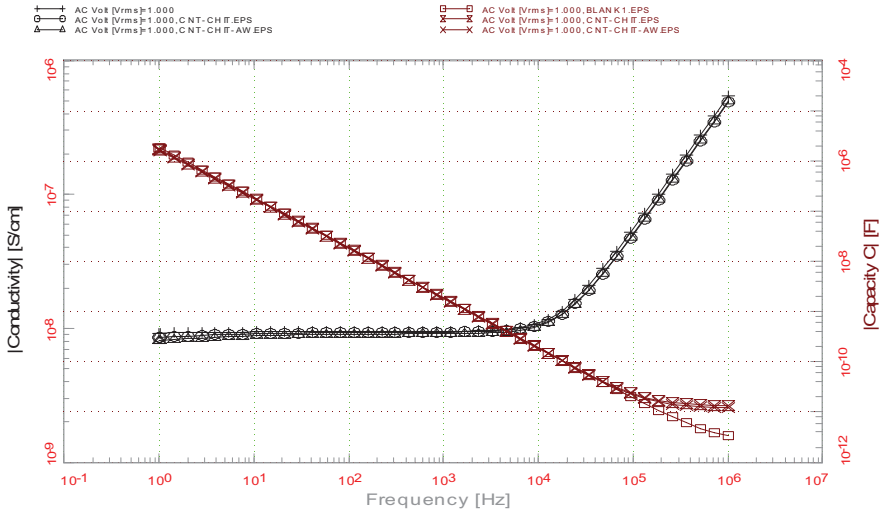

Fig. (3). The variation of parametric conductivities and capacities of the gold, solicon and poly-Si nanogap.

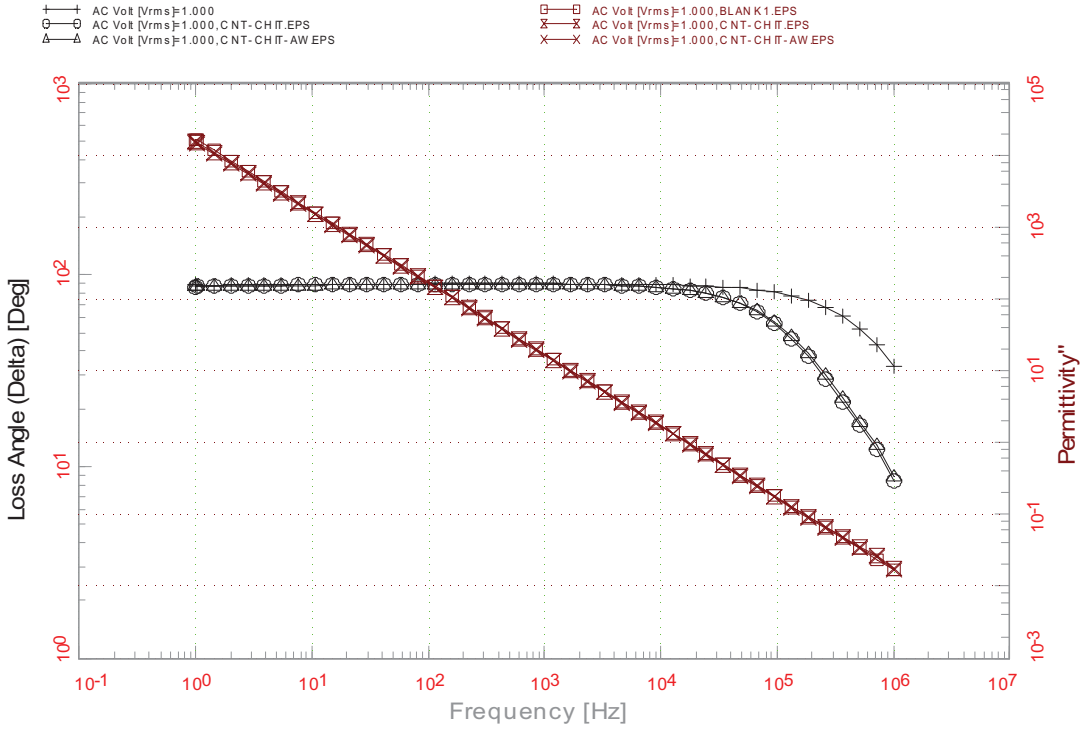

Fig. (4). The relation of loss angle and permittivity for the gold, silicon and poly-Si.

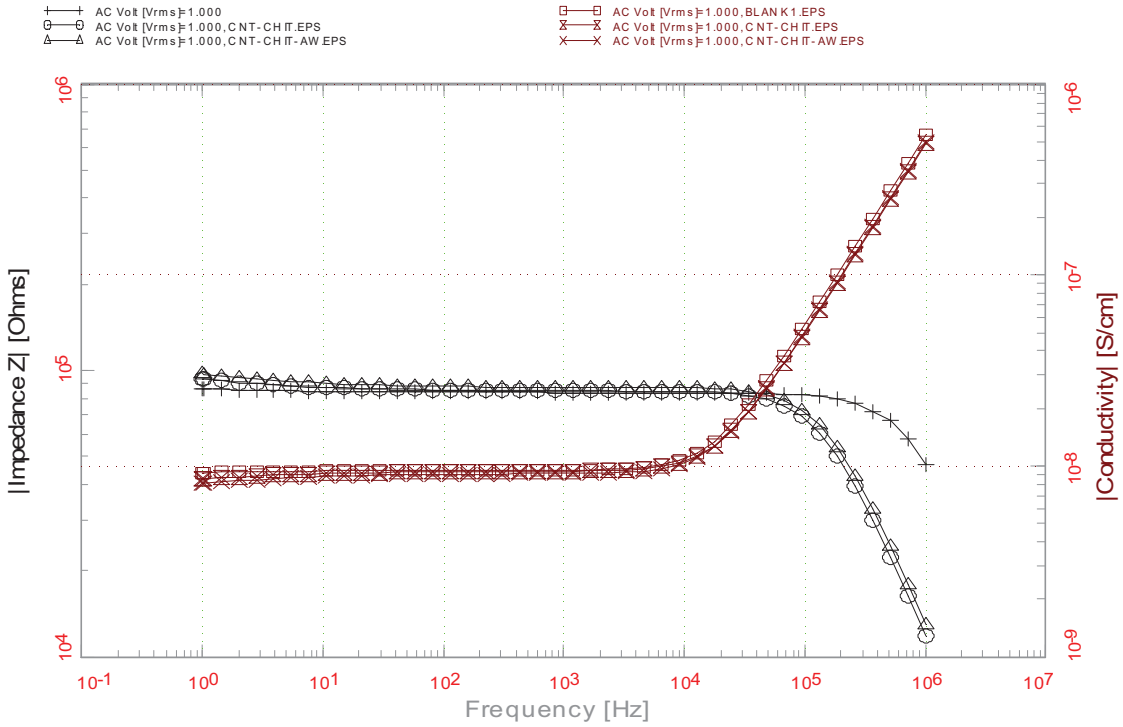

Fig. (5). Impedance and conductivity variation of silicon, gold, and poly-Si nanogap.

material is likely an ohmic contact due to iron formation at the electrodes interface and the ionic conduction through the electrolyte. As expected, at the frequencies higher than 10Khz, the conductance gradually increased.

The design of device was performed by using AUTO-CAD and alignment marks were placed between the device and UV, and for the purpose of fabrication of both device and electrode with ease, the Ti/Au pad fabrication while red line indicates an oxide trench where Si nanogap electrode stands to tune the signal. This was conducted for both silicon and poly-Si materials. However, gold Nanogap fabrication needs additional pre caution because, it cannot be readily fabricated by photolithography, and therefore an additional step is necessary. After cleaning the substrate using ultrasonic machine, EZP520-87 resist is diluted in anisole spin coated at Speed (rpm):4500 (10s), 500 (5s), 0 (5s) to get approximately 100 nm thickness of resist. The resist was baked at 180 ˚C for 2 minutes. With this, the trench pad and gap line are then patterned after development. The trench pads etched separately by using RIE followed by gap line were etched by using DRIE. As a result, a sharp and higher aspect ratio of nanogap was achieved. With the aforementioned steps, nanogaps of 6nm and 90nm were achieved for silicon and poly-silicon nanogaps. Au gold formation is highly challenging because the resist needs to etch lower than micro domain so as to etch the gold using aqua regia, in addition to this challenges its bigger grain size compared to other semiconductor family. However, with care design and systemic resist trimming and etching, it was possible to fabricate the required nanogap size, and to produce more controllable and smaller dimensions of Au nano-gap electrodes a hard mask is necessary, and in this case, aluminum is a good material for this purpose. In this particular study, the employment aluminum was not introduced yet very good gap profile and nanogap sizes were achieved by purely using chemical etching. The recipe for chemical etchant is (HCl 1:3 HN_3). I introduced systematic approach, and for the purpose of fabricating probing units for the silicon and poly-Si device, Ti/Au pad was simply fabricated on top of electrode by using conventional lithographic technique. The measure of gold nanogap electrode was successfully conducted through dielectric analyzer. In metal nanogaps, it can be observed that conductance is extremely high and stable, and it can be assumed that metal nanogaps can lead to extreme field enhancements, nonlocal charge static potential effects and space induced electron tunneling can also be generated. Thus, these properties can be used for sensing both bio and chemical activities that happen at close proximity to device gap. This sensing gap, however, has not been readily exploited due to its behavior under different frequencies and at the same time due to the absence of reliable model to fully understand atomic-scale interaction with the external environment. However, by introducing systematic approach based on electrochemical etching and simple optimization process, we created horizontally arranged arrays of gaps for three different materials including metals, with gap widths as small as between 6nm-9nm nanogaps were achieved

CONCLUSION

The paper demonstrates that in the fabrication and electrical characterization of three nanogap materials, namely: silicon, poly-silicon and gold materials, the gap is in the range of (6 to 9) nm nanogaps. The measure of gold nanogap electrode was successfully conducted through dielectric analyzer. In metal nanogaps it was observed that their conductance is extremely high and stable. It can be assumed that metal nanogaps can lead to extreme field enhancements, nonlocal charge static potential effects and space induced

electron tunneling can also be generated, thus, such properties can be useful for sensing both bio and chemical activities at close proximity to device gap. This sensing gap, however, has not been readily exploited due to its different behavior under different frequencies and at the same time due to the absence of reliable model to fully understand atomic-scale interaction with the external environment. However, by introducing systematic approach based on electrochemical etching and simple optimization process, I created horizontally arranged arrays of gaps for three different materials including metals, with gap widths as small as < 10nm nanogaps and were successfully fabricated and characterized. With this breakthrough, I believe that my proposed approach and findings could lead to the understanding of nanogap devices. Also, I equally believe that nanogap device can be fabricated with ease and in a highly reproducible manner.

CONFLICT OF INTEREST

The authors confirm that this article content has no conflict of interest.

ACKNOWLEDGEMENTS

Declared none.

REFERENCES

[1] David, J.B.; James, S.; Krishnan, J.L.; Amassian, A.; McLachlan, M.A.; Anthopoulos, T.D.; deMello, J.C. Sub-15-nm patterning of asymmetric metal electrodes and devices by adhesion lithography. *Nat. Commun*., **2014**, *5*, 3933.

[2] Kim, J.H.; Moon, H.; Yoo, S.; Choi, Y.K. Nanogap electrode fabrication for a nanoscale device by volume-expanding electrochemical synthesis. *Small*, **2011**, *7*, 2210-2216.

[3] Gao, P.; Zhang, Q.; Li, H.; Chan-Park, M.B. Self-aligned Sub-10-nm nanogap electrode array for large-scale integration. *Small*, **2011**, *7*, 2195-2200.

[4] Ward, D.R.; Huser, F.; Pauly, F.; Cuevas, J.C.; Natelson, D. Optical rectification and field enhancement in a plasmonic nanogap. *Nature,* **2010**, *5*, 732-736.

[5] Singh, B.; Im, H.-N.; Park, J.-Y.; Song, S.-J. Studies on Ionic Conductivity of Sr^{2+}-Doped CeP_2O_7Electrolyte in Humid Atmosphere. *J. Phys. Chem. C*, **2013**, *117*(6), 2653-2661.

[6] Cho, Y.J.; Kim, H.S.; Im, H.; Myung, Y.; Jung, G.B.; Lee, C.W.; Park, J.; Park, M.-H.; Cho, J.; Kang, H.S. Nitrogen-Doped Graphitic Layers Deposited on Silicon Nanowires for Efficient Lithium-Ion Battery Anodes. *J. Phys. Chem. C*, **2011**, *115*(19), 9451-9457.

[7] Fernandez, M.I.; Gonzalez, Y.; Briones, F. Parallel nanogap fabrication with nanometer size control using III-V semiconductor epitaxial technology. *Nanotechnology*, **2008**, *19*(27), 275302.

[8] Haguet, V., Martin, D.; Marcon, L.; Heim, T.; Stiévenard, D.; Olivier, C.; El-Mahdi, O.; Melnyk, O. Combined nanogap nanoparticles nanosensor for electrical detection of biomolecular interactions between polypeptides. *Appl. Phys. Lett*., **2004**, *84*(7), 1213.

[9] Dhahi T.S.; Hashim, U.; Ahmed, N.M.; Eaqub, M.A.; Nazwa, T. Electrical characterization of in-house fabricated polysilicon microgap for yeast concentration measurement. *J. Eng. Technol. Res.*, **2011**, *3*(8), 246-254.

[10] Nazwa, T.; Hashim, U.; Nuzaihan, M.N. Probing the pH Measurement of Self-Alligned Polysilicon Nanogap Capacitor. *Advan. Mater. Res*., **2011**, *364*, 344.

[11] Dhahi T.S.; Hashim, U.; Ahmed, N.M.; Tai, M. A review on the Electrochemical Sensors and Biosensors Composed of Nanogaps as Sensing Material. *J. Optoelectronics Adv. Mater. (JOAM),* **2010**, *12*(29), 1857-1862.

[12] Zhang, Q.; Shenglin, J.; Yike, Z. Dielectric and electric field–induced pyro electric behavior of (Pb0.87−0.07x Ba0.10+0.07x) La0.02 (Zr0.7Sn0.15Ti0.15) O3 ceramics. *J. Mater. Res.*, **2011**, *26*(11), 1436-1440.

[13] Victor, M.; Serdio, V.; Azuma, Y.; Takeshita, S.; Muraki, Taro.; Teranishi, T.; Majima, Y. Robust nanogap electrodes by self-terminating electroless gold plating. *Nanoscale*, **2012**, *4*, 7161-7167.

[14] Nevill, J.T.; Malleo, D. Nanogap Biosensors. *Encyclopedia of Nanotechnology*, **2012**, *2012*, 1544-1552.

Received: March 06, 2015 **Revised: March 24, 2015** **Accepted: April 30, 2015**